

Range-Only Dynamic Output Feedback Controller for Safe and Secure Target Circumnavigation

Anand Singh and Anoop Jain, *Senior Member, IEEE*

Abstract—The safety and security of robotic systems are paramount when navigating around a hostile target. This paper addresses the problem of circumnavigating an unknown target by a unicycle robot while ensuring it maintains a desired safe distance and remains within the sensing region around the target throughout its motion. The proposed control design methodology is based on the construction of a joint Lyapunov function that incorporates: (i) a quadratic potential function characterizing the desired target-circumnavigation objective, and (ii) a barrier Lyapunov function-based potential term to enforce safety and sensing constraints on the robot’s motion. A notable feature of the proposed control design is its reliance exclusively on *local* range measurements between the robot and the target, realized using a dynamic output feedback controller that treats the range as the only observable output for feedback. Using the Lyapunov stability theory, we show that the desired equilibrium of the closed-loop system is asymptotically stable, and the prescribed safety and security constraints are met under the proposed controllers. We also obtain restrictive bounds on the post-design signals and provide both simulation and experimental results to validate the theoretical contributions.

Index Terms—Nonholonomic robot, dynamic output feedback control, barrier Lyapunov function, target circumnavigation.

I. INTRODUCTION

With the increasing sophistication of modern targets, the classical problem of target circumnavigation has garnered significant attention in the control and robotics communities in recent years [1]–[3]. One of the critical aspects in circumnavigating such hostile targets using an autonomous robotic system, such as unmanned aerial vehicle (UAV) or unmanned ground vehicle (UGV), is to restrict its trajectories within a predefined workspace (or region) such that the robot maintains a safe distance from the target while avoiding excessive separation that could disrupt its connection to the target due to sensing limitations. For instance, when tracking an explosive target, a UAV must maintain a safe distance to avoid triggering the explosion while staying within the sensing zone for effective monitoring [4]. Similarly, in scenarios involving hazardous chemical spills, radioactive zones, or critical search areas, a UGV must keep a safe distance to avoid contamination while remaining within the sensing range to maintain contact with the target [5], [6]. Motivated by such applications, we address the problem of safe and secure circumnavigation of an unknown stationary target by a unicycle robot, ensuring its trajectories remain bounded within an annular region around the hostile target. Please note that our use of the terms “safe” and “secure” differs from their usage in the cyber-security

literature [7], which represents a separate research direction beyond the scope of this paper.

During risky target-circumnavigation missions, robots often operate in harsh environments where GPS signals are unreliable or entirely unavailable [8], [9]. In such situations, the robot must rely on local information to achieve target-circumnavigation while adhering to safety and sensing constraints. In this direction, two types of approaches are primarily studied in the literature: (i) the bearing-based approach [2], [3], [10]–[12], and (ii) the range-only-based approach [9], [13]–[17]. The bearing-based approach employs passive sensors, such as cameras or directional antennas, to determine the line-of-sight angle to the target. However, this method does not provide direct measurements of the target’s distance, making it impossible to accurately localize the target with a single measurement [18]. Further, the bearing-based approaches are vulnerable to occlusion and noise in complex environments [19]. On the other hand, the range-only-based approach uses active sensors, such as LiDAR, sonar, or ultrasonic devices, to directly measure the relative distance to the target, and are relatively more precise than bearing-based sensors in GPS-denied areas [20], [21]. Inspired by these practical challenges, this work focuses on solving the target-circumnavigation problem using range-only measurements.

In the literature, an alternate term “range-based” measurements is sometimes used to describe approaches that rely on both range and range-rate information [22]–[24]. From an engineering perspective, range-rate information can be derived from range data using numerical approximation techniques, such as first-order differentiation. However, such estimations introduce noise, cause undesired oscillations, and may even destabilize the system [21], [25]. Although [16] proposed a derivative-free control law, it utilized heading angle as the control input instead of the standard angular velocity. Other works [9], [25] employed second-order sliding mode observers to estimate range-rate, but these methods result in discontinuous controllers with high computational complexity. Some studies [26], [27] derived range-rate information indirectly by exploiting geometrical relationships between range and bearing angles. However, these approaches suffer from reduced accuracy due to their reliance on bearing sensors, as mentioned earlier. Unlike these methods, the proposed work leverages the concept of a dynamic output feedback controller to design a purely range-only-based controller to solve the addressed problem in this paper.

It is noteworthy that none of the aforementioned works address the safety and security aspects of the robot deployed for target circumnavigation, which is the main theme of the pro-

The authors are with the Department of Electrical Engineering, Indian Institute of Technology Jodhpur, 342030, India (e-mail: m23eec001@iitj.ac.in; anoopj@iitj.ac.in).

posed work. While the problem of safe target circumnavigation has been explored in recent literature, existing control designs either rely on bearing measurements and are limited only to the single integrator robot models [2], [3] or require both range and range-rate measurements [28]. To the best of the authors' knowledge, the problem of target-circumnavigation by a nonholonomic unicycle mobile robot with safety and security considerations has not been addressed using range-only measurements. This paper contributes in this direction by leveraging the concept of logarithmic asymmetric barrier Lyapunov functions (ABLFs) [29]. The main contributions and features of this work are summarized as follows:

- *Summary of Contributions:* By introducing a coordinate transformation for the robot-target engagement model, we first propose the controller which uses both range and range-rate information for motivation, followed by the controller which solely relies on the range-only measurements by using the dynamic output feedback design for an unknown target. The control design is based on the construction of a joint Lyapunov function comprising a quadratic potential function V_e , characterizing the desired target-circumnavigation objective, and an ABLF-based potential function V_r , which enforces safety and security constraints on the robot's motion. Specifically, V_e is derived from the transformed relative positional error components between the robot and the target in the Cartesian plane, while V_r is constructed from the robot's positional error relative to the desired circumnavigation radius in polar coordinates. Using the tools from the Lyapunov stability theory, the asymptotic stability of the closed-loop system is rigorously proven, and the robot's trajectories are shown to satisfy the required safety and security constraints under the proposed controllers. Furthermore, restrictive bounds on post-design signals are derived in terms of these potential functions, and the boundedness of the controllers is established. Along with simulations, experimental results using the Khepera IV differential drive ground robot, are provided to illustrate the theoretical findings.
- *Main Features:* The key features of our proposal are three-fold: (a) First, our design approach is free from complex bearing angle analysis, unlike many other works in this direction [9], [21], [26], (ii) Second, no constraints are imposed on the initial heading angle of the navigating robot for assuring its safety and security, unlike [30], [31] which requires both heading angle and position constraints, (iii) Third, the proposed controller allows a large class of (the so-called) *design functions*, including unbounded ones, leading to faster convergence as compared to [13] (which also does not address the safety and security concerns). Note that, despite allowing unbounded design functions, the proposed controllers in our paper remain finite due to the inherent safety and security constraints embedded in the design.

Preliminaries: We denote the set of real numbers by \mathbb{R} , the set of non-negative real numbers by \mathbb{R}_+ , and the n -dimensional real vector space by \mathbb{R}^n . The Euclidean norm of $q \in \mathbb{R}^n$ is represented by $\|q\|$, and the superscript q^\top denotes its transpose. The vector $\mathbf{0}_n \in \mathbb{R}^n$ represents an n -dimensional vector with all components equal to zero. For a differential

map $f : \mathbb{D} \rightarrow \mathbb{R}$, $\mathbb{D} \subset \mathbb{R}^n$, $\nabla_q f = [\partial f / \partial q_1, \dots, \partial f / \partial q_n]^\top$ is the gradient with respect to $q = [q_1, \dots, q_n]^\top \in \mathbb{R}^n$. A continuous, strictly increasing function $\alpha : \mathbb{R}_+ \rightarrow \mathbb{R}_+$ is said to belong to class \mathcal{K}_∞ if $\alpha(0) = 0$ and $\alpha(\bullet) \rightarrow \infty$ as $\bullet \rightarrow \infty$ [32, pg. 144]. Let $\Omega : \mathbb{R} \rightarrow \mathbb{R}$ be a class of smooth functions (now onward referred to as *design functions*) satisfying the properties: (P1) $\Omega(0) = 0$ and $s\Omega(s) > 0$ for $s \neq 0$; (P2) $\alpha_1(|s|) \leq \int_0^s \Omega(\tau) d\tau \leq \alpha_2(|s|)$ for some class \mathcal{K}_∞ functions α_1 and α_2 . Note that it follows from (P1) that $\int_0^s \Omega(\tau) d\tau > 0$ for all $s \neq 0$ and $\int_0^s \Omega(\tau) d\tau = 0$ only if $s = 0$. Examples of such functions include s^n where $n > 0$ is an odd integer, $s/\sqrt{1+s^2}$, $\tanh(s)$, $\arctan(s)$, etc. For clarity, the time argument t is often omitted when evident from the context. Next, we recall barrier Lyapunov function from [29] and highlight an important convergence result that will be helpful in the subsequent analysis.

Definition 1 (Barrier Lyapunov Function (BLF) [29]). *A Barrier Lyapunov Function (BLF) is a scalar function $V(x)$ defined for the state vector $x \in \mathcal{D}$ of the system $\dot{x} = f(x)$ on an open region \mathcal{D} , containing the origin, that is continuous, positive definite, has continuous first-order partial derivatives everywhere in \mathcal{D} , has the property that $V(x) \rightarrow \infty$ as x approaches the boundary of \mathcal{D} , and satisfies $V(x(t)) \leq \varphi$ for all $t \geq 0$, along the solution of $\dot{x} = f(x)$ for $x(0) \in \mathcal{D}$ and some positive constant φ .*

Lemma 1 (Convergence under BLF [29]). *For any positive constants k_a and k_b , let $\mathcal{Z} \triangleq \{\xi \in \mathbb{R} : -k_a < \xi < k_b\} \subset \mathbb{R}$ and $\mathcal{N} \triangleq \mathbb{R}^\ell \times \mathcal{Z} \subset \mathbb{R}^{\ell+1}$ be the open sets. Consider the system $\dot{\eta} = h(t, \eta)$, where $\eta \triangleq [\xi, w]^\top \in \mathcal{N}$, and $h : \mathbb{R}_+ \times \mathcal{N} \rightarrow \mathbb{R}^{\ell+1}$ is piecewise continuous in t and locally Lipschitz in η , uniformly in t , on $\mathbb{R}_+ \times \mathcal{N}$. Suppose there exist functions $U : \mathcal{Z} \rightarrow \mathbb{R}_+$ and $W : \mathbb{R}^\ell \rightarrow \mathbb{R}_+$, continuously differentiable and positive definite in their respective domains, such that $U(\xi) \rightarrow \infty$ as $\xi \rightarrow -k_a$ or $\xi \rightarrow k_b$ and $\gamma_1(\|w\|) \leq W(w) \leq \gamma_2(\|w\|)$ for some class \mathcal{K}_∞ functions γ_1 and γ_2 . Let $V(\eta) \triangleq U(\xi) + W(w)$ and assume that $\xi(0) \in \mathcal{Z}$. If $\dot{V} = (\nabla V)^\top h \leq 0$ holds in the set $\xi \in \mathcal{Z}$, then $\xi(t) \in \mathcal{Z}$ for all $t \in [0, \infty)$.*

II. SYSTEM MODEL, PROBLEM DESCRIPTION AND SOLUTION METHODOLOGY

A. System Model and Problem Description

Consider an under-actuated mobile robot moving in a planar space \mathbb{R}^2 with a nonzero speed $v(t)$, governed by the unicycle kinematic model:

$$\dot{x}(t) = v(t) \cos \theta(t), \quad \dot{y}(t) = v(t) \sin \theta(t), \quad \dot{\theta}(t) = \omega(t), \quad (1)$$

where $[x(t), y(t)]^\top \in \mathbb{R}^2$ is the robot's position and $\theta(t) \in [0, 2\pi)$ is its heading angle in the global (X, Y) -coordinate frame, and $\omega(t) \in \mathbb{R}$ is the turn-rate control input. The objective is to design $\omega(t)$ such that the robot (1) circumnavigates a stationary target T located at position $[x_T, y_T]^\top \in \mathbb{R}^2$ (as shown in Fig. 1). We assume that the robot does not know the position of the target T , instead it can measure the line-of-sight (LoS) distance (or range) to it, denoted as: $r(t) = \sqrt{(x(t) - x_T)^2 + (y(t) - y_T)^2}$.

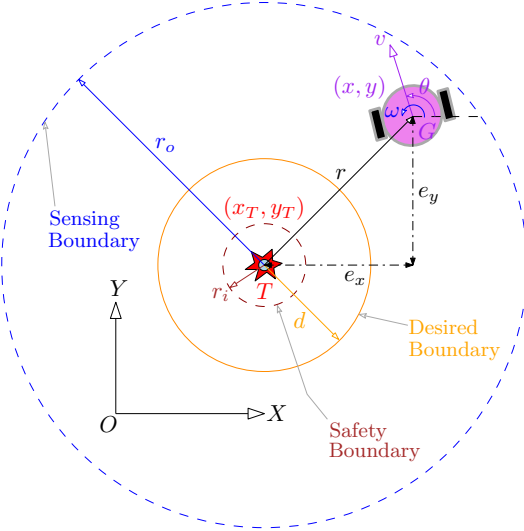


Fig. 1: Safe and secure target circumnavigation by a unicycle robot: An illustration of the problem.

As illustrated in Fig.1, our objective in this paper is to allow the robot to circumnavigate the target T at a constant radial distance d , while assuring that it (a) maintains a safe distance $r_{\text{safe}} := r_i > 0$ from the target, and (b) remains within a desired sensing region defined by the outer radial distance $r_{\text{sensing}} := r_o > 0$, ensuring the target remains within its sensor's coverage. Collectively, it is desired that $r(t) \rightarrow d$ as $t \rightarrow \infty$, and $r_i < r(t) < r_o$ for all $t \geq 0$ where $r_o > r_i$. According to Fig. 1, it is clear that the three radii satisfy the condition $r_i < d < r_o$. It is imperative in the above discussion that the robot must start within the region enclosed by the two radii, that is, $r_i < r(0) < r_o$, which is formally stated in the following assumption:

Assumption 1. For the given inner and outer radii r_i and r_o , respectively, let $\mathcal{Z}_r \triangleq \{r \in \mathbb{R}_+ \mid r_i < r < r_o\}$ be an open set. The robot (1) begins its motion such that $r(0) \in \mathcal{Z}_r$.

It is worth noticing that Assumption 1 places no restrictions on the initial heading angle $\theta(0)$ of the robot (1) and indicates only a natural requirement on its initial positions as in Fig. 1. We now formally state the problem addressed in this paper:

Problem 1. Consider the robot-target engagement as shown in Fig. 1 and assume that the robot (1) begins its motion such that Assumption 1 holds. Design the control law $\omega(t)$ in (1) such that $r(t) \rightarrow d$ as $t \rightarrow \infty$ and $r_i < r(t) < r_o$ for all $t \geq 0$.

B. Solution Methodology

Let $e_x = x - x_T$ and $e_y = y - y_T$ be the positional errors between the robot's geometric center G and target T , as shown in Fig. 1. Using (1), the error dynamics are obtained as $\dot{e}_x = \dot{x} = v \cos \theta$ and $\dot{e}_y = \dot{y} = v \sin \theta$, since $\dot{x}_T = \dot{y}_T = 0$. Notice that the errors $[e_x, e_y]^T$ are uncontrollable as the control ω does not appear in either of the error dynamics. To address this challenge, we solve Problem 1 by proposing

the following coordinate transformation, which maps the error vector $[e_x, e_y]^T$ into a new coordinate frame $[\bar{e}_x, \bar{e}_y]^T$, as:

$$\begin{bmatrix} \bar{e}_x \\ \bar{e}_y \end{bmatrix} = \begin{bmatrix} \cos \theta & \sin \theta \\ -\sin \theta & \cos \theta \end{bmatrix} \begin{bmatrix} e_x \\ e_y \end{bmatrix} + d \begin{bmatrix} 0 \\ 1 \end{bmatrix}. \quad (2)$$

From (2), one can write error dynamics in the transformed coordinates as $\dot{\bar{e}}_x = \dot{e}_x \cos \theta + \dot{e}_y \sin \theta + (e_y \cos \theta - e_x \sin \theta)\dot{\theta}$ and $\dot{\bar{e}}_y = -\dot{e}_x \sin \theta + \dot{e}_y \cos \theta - (e_x \cos \theta + e_y \sin \theta)\dot{\theta}$. Using (1) and (2), these reduce to

$$\dot{\bar{e}}_x = v + (\bar{e}_y - d)\omega \quad (3a)$$

$$\dot{\bar{e}}_y = -\bar{e}_x \omega. \quad (3b)$$

From (3), since it is clear that $[\bar{e}_x, \bar{e}_y]^T$ is controllable, our solution approach focuses on designing the control $\omega(t)$ in the new coordinates to solve Problem 1. Substituting $[e_x, e_y]^T$ in terms of $[\bar{e}_x, \bar{e}_y]^T$ from (2), one can observe that

$$r^2 = e_x^2 + e_y^2 = \bar{e}_x^2 + (\bar{e}_y - d)^2, \quad (4)$$

and the time-derivative of (4), using (2) and (3), is given by:

$$\frac{d}{dt} \left(\frac{1}{2} r^2 \right) = r \dot{r} = (\bar{e}_x \dot{\bar{e}}_x + (\bar{e}_y - d) \dot{\bar{e}}_y) = v \bar{e}_x, \quad (5)$$

which will be useful in the subsequent analysis. From (4), it readily follows that if $[\bar{e}_x, \bar{e}_y]^T \rightarrow \mathbf{0}_2$, $r \rightarrow d$. Note that if the direction of the unit vector $[0, 1]^T \in \mathbb{R}^2$ is reversed in the transformation (2), one gets a similar formulation as in (3) and (4) with a change in the sign of d , which is excluded in our discussion for simplicity. We further introduce the radial error

$$e_r(t) \triangleq r(t) - d, \quad (6)$$

representing the deviation between the robot's position and the radius of the desired circumnavigation path in the polar coordinate. By appropriately constraining the error (6), we aim to satisfy the desired safety and security constraints on the robot's motion. Moreover, $e_r \rightarrow 0 \implies r \rightarrow d$, as desired. Therefore, the equivalent control objectives to Problem 1 is to design controller $\omega(t)$ in (1) such that the transformed errors $[\bar{e}_x, \bar{e}_y]^T \rightarrow \mathbf{0}_2$ as $t \rightarrow \infty$ and $r_i - d < e_r(t) < r_o - d$ (alternatively, $r_i < r(t) < r_o$) for all $t \geq 0$.

III. LYAPUNOV FUNCTIONS AND CONTROL DESIGN

The proposed control design methodology relies on coalition of two Lyapunov functions – (i) one is the quadratic Lyapunov function for minimizing the transformed errors \bar{e}_x and \bar{e}_y to the origin, and (ii) the other is an ABLF associated with the radial error (6) that assures confinement of the radial distance $r(t)$ within the pre-specified safety and sensing bounds. Below, we describe these functions separately, followed by the control design.

A. Constructions of Lyapunov Functions

To minimize errors \bar{e}_x and \bar{e}_y to the origin, we consider the following quadratic Lyapunov function:

$$V_e(\bar{e}_x, \bar{e}_y) = \frac{1}{2}(\bar{e}_x^2 + \bar{e}_y^2), \quad (7)$$

which is positive-definite and attains its minimum value of zero only if $[\bar{e}_x, \bar{e}_y]^\top \rightarrow \mathbf{0}_2$. The time derivative of (7), along the error dynamics (3), is given by

$$\dot{V}_e = \bar{e}_x \dot{\bar{e}}_x + \bar{e}_y \dot{\bar{e}}_y = (v - d\omega)\bar{e}_x. \quad (8)$$

On the other hand, to constrain the range $r(t)$ within the predefined barriers, we propose the following ABLF [29]:

$$V_r(e_r) = \frac{\sigma(e_r)}{2} \ln \left[\frac{\delta_b^2}{\delta_b^2 - e_r^2} \right] + \frac{1 - \sigma(e_r)}{2} \ln \left[\frac{\delta_a^2}{\delta_a^2 - e_r^2} \right], \quad (9)$$

where ‘‘ln’’ denotes the natural logarithm function and $\sigma(e_r)$ is a logic parameter, defined as:

$$\sigma(e_r) \triangleq \begin{cases} 1, & \text{if } e_r > 0, \\ 0, & \text{if } e_r \leq 0. \end{cases} \quad (10)$$

Further, δ_a and δ_b are positive constants and rely on the radii r_i , r_o and d according to the relations:

$$\delta_a = d - r_i, \quad \delta_b = r_o - d. \quad (11)$$

Note that the potential (9) is positive-definite and \mathcal{C}^1 in the domain $e_r \in (-\delta_a, \delta_b)$ (please refer to [29, Lemma 2] for a proof) and $V_r(e_r) = 0$ only if $e_r = 0$. Thus, $V_r(e_r)$ is a valid Lyapunov function candidate in the domain $e_r \in (-\delta_a, \delta_b)$. The time derivative of (9), along the dynamics of (6), is obtained as (note that σ is a logic parameter as in (10)):

$$\dot{V}_r = e_r \dot{e}_r \left[\frac{\sigma(e_r)}{\delta_b^2 - e_r^2} + \frac{1 - \sigma(e_r)}{\delta_a^2 - e_r^2} \right] = (r - d)\dot{r}\eta(e_r), \quad (12)$$

where we denote for simplicity

$$\eta(e_r) \triangleq \frac{\sigma(e_r)}{\delta_b^2 - e_r^2} + \frac{1 - \sigma(e_r)}{\delta_a^2 - e_r^2}. \quad (13)$$

Next, substituting \dot{r} from (5) into (12), we get

$$\dot{V}_r = \left(\frac{r - d}{r} \right) v \bar{e}_x \eta(e_r). \quad (14)$$

Note that e_r is essentially a function of range $r(t)$ (see (6)), and hence, $\eta(e_r)$ in (13). Following this, we will use $\eta(e_r) \triangleq \eta(r)$ interchangeably in the following analysis for simplicity. Next, we discuss the control design.

B. Control Design

In this subsection, we propose the control $\omega(t)$ relying on the potentials (7) and (9), and solve Problem 1. We first describe an approach for motivation where both range and range-rate information are utilized in the control law. We then propose an extension to this control law which uses only the range information and is derived from the dynamic output feedback control approach.

1) *Availability of range and range-rate measurements:* When both range and range rate are available, we have the following result:

Theorem 1. *Consider the robot-target engagement shown in Fig. 1 and assume that Assumption 1 holds. Let the robot (1) be governed by the control law*

$$\omega(t) = \frac{v}{d} + vk_1 \Omega(r\dot{r}) + vk_2 \left(\frac{r - d}{r} \right) \eta(r), \quad (15)$$

where $k_1 > 0$ and $k_2 > 0$ are the control gains, and $\Omega(\bullet)$ is the design function (introduced in the preliminaries). Then, $r_i < r(t) < r_o$ for all $t \geq 0$, and $\bar{e}_x(t) = \bar{e}_y(t) \rightarrow 0$ and $r(t) \rightarrow d$ as $t \rightarrow \infty$ in the set \mathcal{Z}_r .

Proof. Consider the joint candidate Lyapunov function

$$V_1(\bar{e}_x, \bar{e}_y, e_r) = V_e(\bar{e}_x, \bar{e}_y) + dk_2 V_r(e_r), \quad (16)$$

where V_e and V_r are defined in (7) and (9), respectively. Using (8) and (14), the time derivative of (16) is given by:

$$\dot{V}_1 = (v - d\omega)\bar{e}_x + dk_2 \left(\frac{r - d}{r} \right) v \bar{e}_x \eta(r). \quad (17)$$

Further, using (5), the control (15) can be written as:

$$\omega = \frac{v}{d} + vk_1 \Omega(v\bar{e}_x) + vk_2 \left(\frac{r - d}{r} \right) \eta(r), \quad (18)$$

which, upon substitution into (17) and simplification, yields

$$\dot{V}_1 = -dk_1 (v\bar{e}_x) \Omega(v\bar{e}_x). \quad (19)$$

Since $d > 0$, $k_1 > 0$ and $\Omega(\bullet)$ satisfies property (P1) from the preliminaries, we conclude that \dot{V}_1 is negative semi-definite, i.e., $\dot{V}_1 \leq 0$. As Assumption 1 holds, it now immediately follows from Lemma 1 that $-\delta_a < e_r(t) < \delta_b$ for all $t \geq 0$ in the set \mathcal{Z}_r , since the potential $V_r \rightarrow \infty$ as $e_r \rightarrow -\delta_a$ or $e_r \rightarrow \delta_b$ and $c_1(\bar{e}_x^2 + \bar{e}_y^2) \leq V_e \leq c_2(\bar{e}_x^2 + \bar{e}_y^2)$ for some constants $c_1 \in [0, 1/2]$ and $c_2 \in [1/2, \infty)$. Substituting for δ_a and δ_b from (11), and $e_r(t)$ from (6), the preceding error inequality $-\delta_a < e_r(t) < \delta_b$ implies that $r_i < r(t) < r_o$ for all $t \geq 0$ in \mathcal{Z}_r . This proves the first statement.

To prove the second statement, notice that $V_1(\bar{e}_x, \bar{e}_y, e_r) \leq V_1(\bar{e}_x(0), \bar{e}_y(0), e_r(0))$ for all $t \geq 0$ in \mathcal{Z}_r , because $\dot{V}_1 \leq 0$. Further, it is straightforward to see that $V_1(\bar{e}_x(0), \bar{e}_y(0), e_r(0))$ is finite and positive for any given initial conditions in \mathcal{Z}_r . In other words, it implies that there exists a positive constant λ_1 such that $V_1(\bar{e}_x, \bar{e}_y, e_r) \leq \lambda_1$ for all initial conditions in \mathcal{Z}_r . Note that the set $\Lambda_1 \triangleq \{[\bar{e}_x, \bar{e}_y, e_r]^\top \in \mathbb{R}^2 \times (-\delta_a, \delta_b) \mid V_1(\bar{e}_x, \bar{e}_y, e_r) \leq \lambda_1\}$ is compact and positively invariant, since V_1 is positive definite and continuously differentiable, and $\dot{V}_1 \leq 0$ in \mathcal{Z}_r . From LaSalle’s invariance principle [32, Theorem 4.4, pg. 128], it follows that all the trajectories of (1) and (3) converge to the largest invariant set Δ_1 contained in the set $\Gamma_1 \triangleq \{[\bar{e}_x, \bar{e}_y, e_r] \in \mathbb{R}^2 \times (-\delta_a, \delta_b) \mid \dot{V}_1 = 0\} \subset \Lambda_1$ as $t \rightarrow \infty$. Notice that $\dot{V}_1 = 0$ only if $v\bar{e}_x = 0 \implies \bar{e}_x = 0$, as $v \neq 0$ (see (19)). That is, $\bar{e}_x = \dot{\bar{e}}_x = 0$ in Γ_1 , which on substitution in (3), gives

$$v + (\bar{e}_y - d)\omega = 0, \quad (20)$$

and $\dot{\bar{e}}_y = 0$, which implies that \bar{e}_y is constant, and so is, $\bar{e}_y - d$ in Γ_1 (as d is fixed). Note that $\bar{e}_y - d \neq 0$ in Γ_1 , as if $\bar{e}_y - d = 0$, $r = 0$ in Γ_1 according to (4), which is a contradiction since $r_i < r(t) < r_o$ for all $t \geq 0$ in \mathcal{Z}_r , as proved in the first statement. Consequently, it follows from (4) that $r(t) = r_c$ as $t \rightarrow \infty$ in Γ_1 where $r_c \in (r_i, r_o)$ is a constant. This implies that the robot (1) moves on a circular path with angular velocity $\omega = v/r_c$ in Γ_1 as $t \rightarrow \infty$. Substituting $\omega = v/r_c$ into (18) and simplifying in Γ_1 , we get $(v/r_c) = (v/d) +$

$vk_2((r_c - d)/r_c)\eta(r_c)$, which reduces to the condition

$$(r_c - d)(1 + dk_2\eta(r_c)) = 0. \quad (21)$$

From (13), it can be easily verified that $\eta(e_r) > 0$ for $e_r \in (-\delta_a, \delta_b)$, and hence, $1 + dk_2\eta(r_c) > 0$ in Γ_1 . Therefore, (21) holds only if $r_c = d$, that is, the robot moves around the circular trajectory of the desired radius d with the angular rate $\omega = v/d$ in Γ_1 as $t \rightarrow \infty$. Now, using (20), one can conclude that $\bar{e}_y = 0$ as $t \rightarrow \infty$ in Γ_1 . Consequently, it follows that the largest invariant set $\Delta_1 \subset \Gamma_1 \subset \Lambda_1$ contains only the desired equilibrium where $\bar{e}_x(t) = \bar{e}_y(t) \rightarrow 0$, and $r(t) \rightarrow d$, as $t \rightarrow \infty$. This concludes the proof. \square

Please note that in the above proof, the set Γ_1 is well-defined because \dot{V}_1 in (19) and the potential $V_1(\bar{e}_x, \bar{e}_y, e_r)$ in (16) do not show any explicit dependence on time t , since the speed profile $v(t)$ is assumed to be nonzero (i.e., it is chosen to be either positive or negative for all time $t \geq 0$). This feature allows the use of LaSalle's invariance principle to prove the asymptotic stability of the closed-loop system, rather than relying on Barbalat's lemma (please refer to [32, pp. 323–325]).

2) *Availability of range-only measurements:* In control law (15), notice that only the term $\Omega(r\dot{r})$ is dependent on the range rate \dot{r} . Our approach here is to modify the argument $r\dot{r}$ of the design function Ω via a term that is solely dependent on the range information and assures the stability of the desired equilibrium of the closed-loop stability. In this direction, we use the output dynamic feedback approach [13] where we designate $y = (1/2)r^2$ as the output and propose the following variation of the control law (15):

$$\omega = \frac{v}{d} + vk_1\Omega(-\kappa z + y) + vk_2\left(\frac{r-d}{r}\right)\eta(r) \quad (22a)$$

$$\dot{z} = -\kappa z + y, \quad (22b)$$

where $\kappa > 0$ is a gain term. Note that in the revised control law (22a) our approach is to estimate $r\dot{r}$ using only the range r and an auxiliary variable $z \in \mathbb{R}$ with dynamics (22b). For further analysis, we denote $\beta \triangleq -\kappa z + y$. Using (5), the time derivative of β is obtained as:

$$\dot{\beta} = -\kappa\dot{z} + r\dot{r} = -\kappa\beta + v\bar{e}_x. \quad (23)$$

Further, the resultant error dynamics (3), under the control (22), can be written as:

$$\begin{aligned} \dot{\bar{e}}_x &= v + (\bar{e}_y - d) \left[\frac{v}{d} + vk_1\Omega(\beta) + vk_2\left(\frac{r-d}{r}\right)\eta(r) \right] \\ &= \frac{v\bar{e}_y}{d} + (\bar{e}_y - d) \left[vk_1\Omega(\beta) + vk_2\left(\frac{r-d}{r}\right)\eta(r) \right] \end{aligned} \quad (24a)$$

$$\dot{\bar{e}}_y = -\bar{e}_x \left[\frac{v}{d} + vk_1\Omega(\beta) + vk_2\left(\frac{r-d}{r}\right)\eta(r) \right]. \quad (24b)$$

We have the following result:

Theorem 2. *Consider the robot-target engagement shown in Fig. 1 and assume that Assumption 1 holds. Let the robot (1) be governed by the control law (22). Then, $r_i < r(t) < r_o$ for*

all $t \geq 0$, and $\bar{e}_x(t) = \bar{e}_y(t) = \beta(t) \rightarrow 0$ and $r(t) \rightarrow d$ as $t \rightarrow \infty$ in the set \mathcal{Z}_r .

Proof. Consider the following candidate Lyapunov function

$$V_2(\bar{e}_x, \bar{e}_y, e_r, \beta) = V_1(\bar{e}_x, \bar{e}_y, e_r) + dk_1 \int_0^\beta \Omega(\tau) d\tau, \quad (25)$$

where V_1 is given by (16). Note that V_2 is positive-definite and satisfies all the requirements indicated in Lemma 1 because of the properties of the design function Ω , defined in the preliminaries. Following the steps similar to the proof of Theorem 1, the time derivative of (16), along the new error dynamics (24), is obtained as $\dot{V}_1 = -dk_1(v\bar{e}_x)\Omega(\beta)$. Therefore, the time derivative of (25), along the new error dynamics (24), is given by $\dot{V}_2 = -dk_1(v\bar{e}_x)\Omega(\beta) + dk_1\dot{\beta}\Omega(\beta)$. Now, using (23), we have

$$\begin{aligned} \dot{V}_2 &= -dk_1(v\bar{e}_x)\Omega(\beta) + dk_1(-\kappa\beta + v\bar{e}_x)\Omega(\beta) \\ &= -d\kappa k_1\beta\Omega(\beta). \end{aligned} \quad (26)$$

Since $\dot{V}_2 \leq 0$ and Assumption 1 holds, it immediately follows from Lemma 1 that $r_i < r(t) < r_o$ for all $t \geq 0$ in \mathcal{Z}_r (similar to the proof of Theorem 1). Along the similar steps, one can further conclude that there exists a positive constant λ_2 such that $V_2(\bar{e}_x, \bar{e}_y, e_r, \beta) \leq \lambda_2$ for all initial conditions in \mathcal{Z}_r . Note that the set $\Lambda_2 \triangleq \{[\bar{e}_x, \bar{e}_y, e_r, \beta]^T \in \mathbb{R}^2 \times (-\delta_a, \delta_b) \times \mathbb{R} \mid V_2(\bar{e}_x, \bar{e}_y, e_r, \beta) \leq \lambda_2\}$ is compact and positively invariant, since V_2 is positive definite and continuously differentiable, and $\dot{V}_2 \leq 0$ in \mathcal{Z}_r . Now, using LaSalle's invariance principle [32, Theorem 4.4, pg. 128], it can be concluded that all the trajectories of (1) converge to the largest invariant set Δ_2 contained in the set $\Gamma_2 \triangleq \{[\bar{e}_x, \bar{e}_y, e_r, \beta]^T \mid \dot{V}_2 = 0\} \subset \Lambda_2$ as $t \rightarrow \infty$. From (26), note that $\dot{V}_2 = 0$ only if $\beta = 0$. That is, $\beta = \dot{\beta} = 0$ in Γ_2 , which on substitution in (23), gives $v\bar{e}_x = 0 \implies \bar{e}_x = 0$ (hence $\dot{\bar{e}}_x = 0$) in Γ_2 as $v \neq 0$. Now, the remaining analysis follows the same reasoning as in the proof of Theorem 1, and hence, omitted for brevity. Consequently, it follows that the largest invariant set $\Delta_2 \subset \Gamma_2 \subset \Lambda_2$ contains only the desired equilibrium where $\bar{e}_x(t) = \bar{e}_y(t) = \beta(t) \rightarrow 0$, and $r(t) \rightarrow d$, as $t \rightarrow \infty$. This concludes the proof. \square

Remark 1. *Unlike the control law (15), the controller (22) relies solely on range-based measurements and an auxiliary dynamic variable z , which can be initialized arbitrarily. It is important to highlight that our approach is based only on the natural assumption on the initial range $r(0)$, as stated in Assumption 1; we do not impose any requirements on the initial heading angle $\theta(0)$ of the robot model (1), unlike [30] where the initial conditions must be appropriately chosen for both $r(0)$ and $\theta(0)$ and the control implementation requires both $r(t)$ and $\theta(t)$ information. Further, the design function Ω in controllers (15) and (22) accommodates a large class of functions, including unbounded ones, as per its properties (P1) and (P2) in the preliminaries, unlike [13], which does not account for such generality in design functions. These are two major features of our work, along with the consideration of both safe and sensing constraints.*

IV. ANALYSIS OF POST-DESIGN SIGNALS

Exploiting the potentials (16) and (25), this section obtains the bounds on the radial error $e_r(t)$ and the range $r(t)$ in a restricted sense and also shows the boundedness of the proposed controllers (15) and (22). In this direction, we present the following two theorems corresponding to the above cases of availability/non-availability of the range-rate information.

Theorem 3 (Availability of range and range-rate measurements). *Under the conditions given in Theorem 1, the following statements hold for all $t \geq 0$ within the set \mathcal{Z}_r :*

(a) *The squared norm of the transform error vector $[\bar{e}_x(t), \bar{e}_y(t)]^\top$ satisfies:*

$$\bar{e}_x^2(t) + \bar{e}_y^2(t) \leq (\sqrt{2V_1(0)})^2, \quad (27)$$

where $V_1(0) \triangleq V_1(\bar{e}_x(0), \bar{e}_y(0), e_r(0))$, obtained from (16) at $t = 0$.

(b) *The radial error $e_r(t)$ and the range $r(t)$ belong to the following compact sets:*

$$e_r(t) \in [-\delta_a \Upsilon_1, \delta_b \Upsilon_1], \quad (28a)$$

$$r(t) \in [r_i + \delta_a(1 - \Upsilon_1), r_o - \delta_b(1 - \Upsilon_1)], \quad (28b)$$

where $\Upsilon_1 = \sqrt{1 - e^{-(2/dk_2)V_1(0)}}$ is a constant.

Proof. Since $\dot{V}_1 \leq 0$ in \mathcal{Z}_r , $V_1(\bar{e}_x(t), \bar{e}_y(t), e_r(t)) \leq V_1(0)$ for all $t \geq 0$ in \mathcal{Z}_r . Consequently, it follows from (16) that $V_e(\bar{e}_x, \bar{e}_y) \leq V_1(0)$ and $dk_2 V_r(e_r) \leq V_1(0)$ for all $t \geq 0$ in \mathcal{Z}_r . Now, substituting for V_e and V_r from (7) and (9), respectively, the preceding inequalities imply $\bar{e}_x^2 + \bar{e}_y^2 \leq (\sqrt{2V_1(0)})^2$, proving the first result, and

$$\frac{1}{dk_2} V_1(0) \geq \begin{cases} \frac{1}{2} \ln \left[\frac{\delta_b^2}{\delta_b^2 - e_r^2(t)} \right], & \text{if } 0 < e_r(t) < \delta_b \\ \frac{1}{2} \ln \left[\frac{\delta_a^2}{\delta_a^2 - e_r^2(t)} \right], & \text{if } -\delta_a < e_r(t) \leq 0, \end{cases} \quad (29)$$

for all $t \geq 0$ in \mathcal{Z}_r . Taking exponential on both sides of (29), yields

$$e_r^2(t) \leq \begin{cases} \delta_b^2(1 - e^{-(2/dk_2)V_1(0)}), & \text{if } 0 < e_r(t) < \delta_b, \\ \delta_a^2(1 - e^{-(2/dk_2)V_1(0)}), & \text{if } -\delta_a < e_r(t) \leq 0. \end{cases}$$

By taking square root on both sides of the above inequality, we obtain $e_r(t) \leq \delta_b \sqrt{1 - e^{-(2/dk_2)V_1(0)}}$ for $e_r(t) \in (0, \delta_b)$ and $e_r(t) \geq -\delta_a \sqrt{1 - e^{-(2/dk_2)V_1(0)}}$ for $e_r(t) \in (-\delta_a, 0]$. By combining both, it follows that $-\delta_a \sqrt{1 - e^{-(2/dk_2)V_1(0)}} \leq e_r(t) \leq \delta_b \sqrt{1 - e^{-(2/dk_2)V_1(0)}}$ for all $t \geq 0$ in \mathcal{Z}_r . Further, substituting for $e_r(t)$ from (6) and using (11), we can get $r_i + \delta_a[1 - \sqrt{1 - e^{-(2/dk_2)V_1(0)}}] \leq r(t) \leq r_o - \delta_b[1 - \sqrt{1 - e^{-(2/dk_2)V_1(0)}}]$ for all $t \geq 0$ in \mathcal{Z}_r . This proves the second claim. \square

Theorem 4 (Availability of range-only measurements). *Under the conditions given in Theorem 2, the following statements hold for all $t \geq 0$ within the set \mathcal{Z}_r :*

(a) *The squared norm of the transform error vector $[\bar{e}_x(t), \bar{e}_y(t)]^\top$ satisfies the following:*

$$\bar{e}_x^2(t) + \bar{e}_y^2(t) \leq (\sqrt{2V_2(0)})^2, \quad (30)$$

where $V_2(0) \triangleq V_2(\bar{e}_x(0), \bar{e}_y(0), e_r(0), \beta(0))$, obtained from (25) at $t = 0$.

(b) *The radial error $e_r(t)$ and the range $r(t)$ belong to the following compact sets:*

$$e_r(t) \in [-\delta_a \Upsilon_2, \delta_b \Upsilon_2], \quad (31a)$$

$$r(t) \in [r_i + \delta_a(1 - \Upsilon_2), r_o - \delta_b(1 - \Upsilon_2)], \quad (31b)$$

where $\Upsilon_2 = \sqrt{1 - e^{-(2/dk_2)V_2(0)}}$ is a constant.

(c) *The modulus of the signal $\beta(t)$ in (23) remains bounded by*

$$|\beta(t)| \leq \alpha_1^{-1} \left(\frac{V_2(0)}{dk_1} \right), \quad (32)$$

for some class \mathcal{K}_∞ function α_1 , satisfying the property (P2) of the design function Ω .

(d) *The modulus of the auxiliary signal $z(t)$ in (22b) remains bounded by $\underline{\chi} \leq |z(t)| \leq \bar{\chi}$, where*

$$\underline{\chi} = \frac{1}{\kappa} \left[\frac{1}{2} (r_i + \delta_a(1 - \Upsilon_2))^2 - \alpha_1^{-1} \left(\frac{V_2(0)}{dk_1} \right) \right], \quad (33a)$$

$$\bar{\chi} = \frac{1}{\kappa} \left[\frac{1}{2} (r_o - \delta_b(1 - \Upsilon_2))^2 + \alpha_1^{-1} \left(\frac{V_2(0)}{dk_1} \right) \right]. \quad (33b)$$

Proof. Since $\dot{V}_2 \leq 0$ in \mathcal{Z}_r from (26), the proof of part (a) and part (b) follows along the similar steps as in Theorem 3 by replacing $V_1(0)$ by $V_2(0)$, and hence, is omitted for brevity. To prove part (c), one can apply the same reasoning (as in the above proof) and infer from (25) that $dk_1 \int_0^\beta \Omega(\tau) d\tau \leq V_2(0)$ for all $t \geq 0$ in \mathcal{Z}_r . Exploiting the property (P2) of the design function Ω , it can be concluded that $\alpha_1(|\beta(t)|) \leq \int_0^\beta \Omega(\tau) d\tau \leq V_2(0)/dk_1$ for some class \mathcal{K}_∞ function α_1 for all $t \geq 0$ in \mathcal{Z}_r . Alternatively, $\alpha_1(|\beta(t)|) \leq V_2(0)/dk_1 \implies |\beta(t)| \leq \alpha_1^{-1}(V_2(0)/dk_1)$ for all $t \geq 0$ in \mathcal{Z}_r . Further, to prove part (d), replacing $\beta(t) = -\kappa z(t) + y(t)$ in the preceding inequality, implies $|\kappa z(t) + y(t)| \leq \alpha_1^{-1}(V_2(0)/dk_1)$. Since $|\kappa z| - |y| \leq |-\kappa z + y|$, it follows from the former inequality that $|\kappa z(t) - |y(t)|| \leq \alpha_1^{-1}(V_2(0)/dk_1)$, which implies that $\frac{1}{\kappa} [|y(t)| - \alpha_1^{-1} \left(\frac{V_2(0)}{dk_1} \right)] \leq |z(t)| \leq \frac{1}{\kappa} [|y(t)| + \alpha_1^{-1} \left(\frac{V_2(0)}{dk_1} \right)]$ for all $t \geq 0$ in \mathcal{Z}_r . Since $y = (1/2)r^2$, it follows from (31b) that $\frac{1}{2}(r_i + \delta_a(1 - \Upsilon_2))^2 \leq |y(t)| \leq \frac{1}{2}(r_o - \delta_b(1 - \Upsilon_2))^2$ for all $t \geq 0$ in \mathcal{Z}_r . Consequently, the result follows after applying the preceding bounds on $|y(t)|$. This completes the proof. \square

Remark 2 (Boundedness of proposed controllers). *Note that the controls (15) and (22) remain bounded along any solution trajectory within the set \mathcal{Z}_r , because of the following: (i) the term $\eta(r)$, given by (13), is finite since $-\delta_a < e_r(t) < \delta_b$ for all $t \geq 0$ in \mathcal{Z}_r , as established in Theorem 1 and Theorem 2, (ii) the design function Ω remains finite due to its bounded argument for all $t \geq 0$ in \mathcal{Z}_r in both the cases: (a) For controller (15), the boundedness of $\Omega(r\dot{r})$ follows from the fact that \bar{e}_x is bounded from (27), and so is $r\dot{r}$, using (5). (b) For controller (22), the boundedness of $\Omega(-\kappa z + y) = \Omega(\beta)$ follows from (32).*

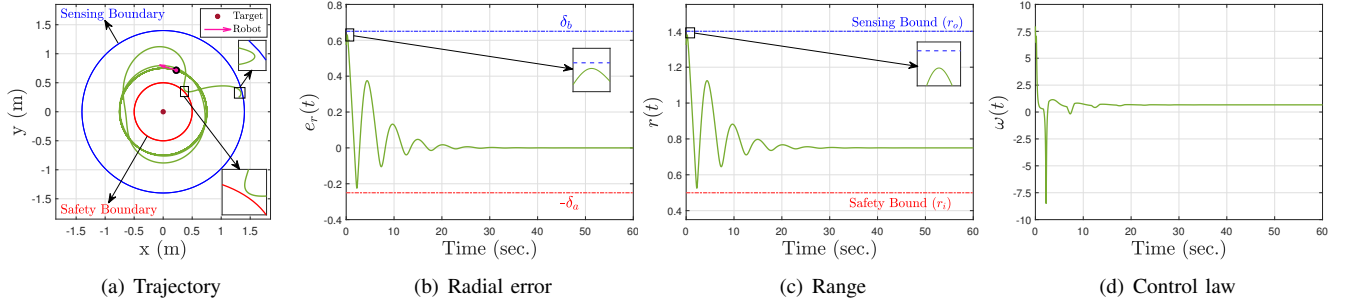


Fig. 2: Robot's trajectory and time evolution of radial error (6), range and control law (22a) under range-only controller (22).

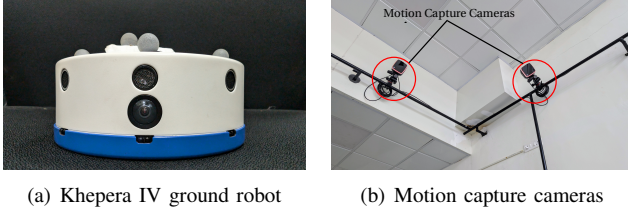


Fig. 3: Khepera IV robot and MoCap validation setup.

V. SIMULATION AND EXPERIMENTAL RESULTS

In principle, our approach is applicable even if the robot begins arbitrarily close to the two boundaries, provided Assumption 1 holds. However, in practice, a real robotic system must be initialized with a sufficient safety margin to account for its physical structure. We illustrate both these aspects through simulations and experiments as follows:

A. Simulations

Consider a robot moving at a constant speed of $v = 0.5$ (m/s) with an initial position and heading angle of $[x(0), y(0)]^T = [1.3, 0.25]^T$ (m) and $\theta(0) = 25^\circ$, respectively. Let the robot be deployed to circumnavigate the target T , located at $[x_T, y_T]^T = [0, 0]^T$, at a desired radius $d = 0.75$ (m), while satisfying safety and sensing constraints with $r_i = 0.5$ (m) and $r_o = 1.4$ (m), respectively. Clearly, Assumption 1 is satisfied, since $r_i = 0.5 < r(0) = 1.3238 < r_o = 1.4$. Using (11), the barriers are obtained as $\delta_a = d - r_i = 0.25$ and $\delta_b = r_o - d = 0.65$. Assuming a linear design function $\Omega(\tau) = \tau$ for simplicity, we simulated the range-only controller (22) with control gains $k_1 = 14$, $k_2 = 0.5$, $\kappa = 7$, initializing the auxiliary variable as $z(0) = 0$ (the results for control (15) are omitted for brevity). The results are plotted in Fig. 2 where Fig. 2(a) shows that the robot circumnavigates the target at the desired distance and successfully satisfies both the safety and sensing constraints. Fig. 2(b) and Fig. 2(c) depict the time evolution of the radial error $e_r(t)$ and the range $r(t)$, respectively. These satisfy their respective bounds as obtained in Theorem 2 and eventually approach their desired values. Fig. 2(d) plots the time evolution of the controller (22a) which approaches the steady state value of $v/d \approx 0.67$ (rad/s), as desired.

B. Experiments

We performed experiments using a *Khepera IV* differential-drive ground robot (see Fig. 3(a)) with the help of a motion capture (MoCap) validation setup comprising overhead cameras (see Fig. 3(b)). The MoCap system is operated via a task manager where the data is recorded and processed for feedback. We considered that the *Khepera IV* begins with the initial position and heading angle of $[x(0), y(0)]^T = [1.05, 0.20]^T$ and $\theta(0) = 90^\circ$, respectively (satisfying Assumption 1 for the same boundary constraints as in simulation subsection). Since *Khepera* is a differential drive robot, we obtained the speeds v_ℓ and v_r of its left and right vehicles from the linear and angular speeds of the (unicycle) robot (1) as follows: $v_r = v + (d_w/2)\omega$, $v_\ell = v - (d_w/2)\omega$ where $d_w = 10.54$ (cm) is the distance between the two wheels of *Khepera* robot. The robot was operated at a constant linear speed $v = 0.5$ (m/s), following the hardware limit of maximum wheel speed of 0.814 (m/s). Upon implementing the controller (22) with control gains $k_1 = 3$, $k_2 = 1$, $\kappa = 4$, we captured the experimental results as shown in Fig. 4. Fig. 4(a) provides a top-down view of the robot's motion, highlighting its position at $t = 26$ seconds. The robot's path, recorded throughout the experiment from the task manager, is illustrated in Fig. 4(b). Further, Fig. 4(c) and Fig. 4(d) display the range and the performance of the controller (22a), respectively. The video of the conducted experiments can be found on <https://youtu.be/XoNbWddjNvY>.

VI. CONCLUSION AND FUTURE REMARKS

Using the concepts of the range-based dynamic output feedback controller and ABLF, this paper investigated the problem of safe and secure circumnavigation of a hostile target by a unicycle robot. The proposed controller relied exclusively on range measurements and ensured that the robot's trajectories remained bounded within a predefined annular region around the target by appropriately selecting the barriers δ_a and δ_b . The (local) asymptotic stability of the closed-loop system was rigorously established, and analytical bounds were obtained for various intermediate signals, including the proposed controllers. The core of the control design lied in effectively combining the two potential functions (7) and (9). It is worth noticing that both these potentials minimize at the desired equilibrium where $r \rightarrow d$, however, none of these individually can guarantee both the objectives simultaneously,

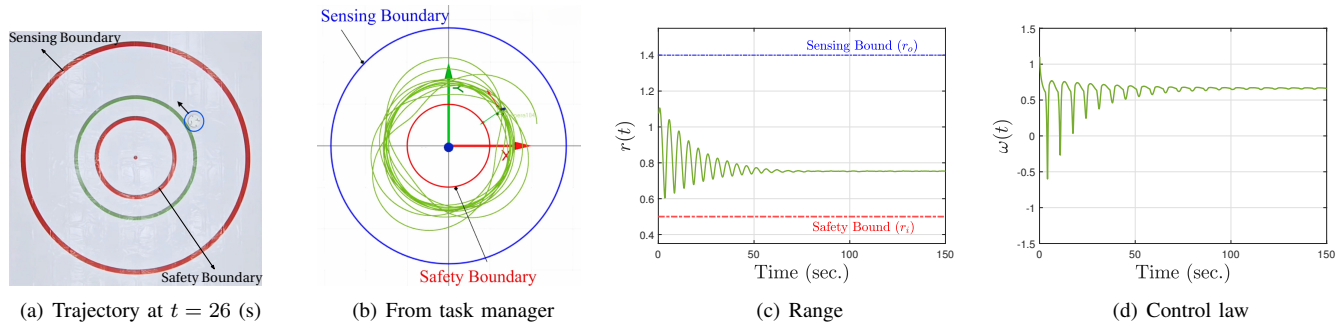


Fig. 4: Experimental results for Khepera IV robot using range only measurements.

as: (i) (7) does not account for the desired safety and sensing constraints, (ii) (9) does fulfill both the stabilizing and constraints requirements, it alone cannot be used for control design, since its derivative (12) depends on \dot{r} which is not (directly) controllable via ω (see (4)). Hence, both potentials are necessary.

There is a wide scope for future research in this direction, including the consideration of moving targets, the presence of arbitrary-shaped boundary constraints, an extension of the problem to the 3D scenario, and multi-agent safe and secure target circumnavigation problems.

REFERENCES

- [1] R. Sharma, M. Kothari, C. N. Taylor, and I. Postlethwaite, "Cooperative target-capturing with inaccurate target information," in *Proceedings of the 2010 American Control Conference*. IEEE, 2010, pp. 5520–5525.
- [2] S. Cao, R. Li, Y. Shi, and Y. Song, "Safe convex-circumnavigation of one agent around multiple targets using bearing-only measurements," *Automatica*, vol. 134, p. 109934, 2021.
- [3] R. Li, Y. Shi, X. Wu, and Y. Song, "Safe-circumnavigation of one single agent around a group of targets with only bearing information," *Journal of the Franklin Institute*, vol. 356, no. 18, pp. 11 546–11 560, 2019.
- [4] U. Zengin and A. Dogan, "Real-time target tracking for autonomous uavs in adversarial environments: A gradient search algorithm," *IEEE Transactions on Robotics*, vol. 23, no. 2, pp. 294–307, 2007.
- [5] L. Brinón-Arranz, L. Schenato, and A. Seuret, "Distributed source seeking via a circular formation of agents under communication constraints," *IEEE Transactions on Control of Network Systems*, vol. 3, no. 2, pp. 104–115, 2015.
- [6] M. A. Demetriou and E. Bakolas, "Navigating over 3d environments while minimizing cumulative exposure to hazardous fields," *Automatica*, vol. 115, p. 108859, 2020.
- [7] A. Teixeira, I. Shames, H. Sandberg, and K. H. Johansson, "A secure control framework for resource-limited adversaries," *Automatica*, vol. 51, pp. 135–148, 2015.
- [8] H. Qin, Z. Meng, W. Meng, X. Chen, H. Sun, F. Lin, and M. H. Ang, "Autonomous exploration and mapping system using heterogeneous uavs and ugvs in gps-denied environments," *IEEE Transactions on Vehicular Technology*, vol. 68, no. 2, pp. 1339–1350, 2019.
- [9] Y. Cao, "Uav circumnavigating an unknown target under a gps-denied environment with range-only measurements," *Automatica*, vol. 55, pp. 150–158, 2015.
- [10] M. Deghat, I. Shames, B. D. Anderson, and C. Yu, "Localization and circumnavigation of a slowly moving target using bearing measurements," *IEEE Transactions on Automatic Control*, vol. 59, no. 8, pp. 2182–2188, 2014.
- [11] R. Zheng, Y. Liu, and D. Sun, "Enclosing a target by nonholonomic mobile robots with bearing-only measurements," *Automatica*, vol. 53, pp. 400–407, 2015.
- [12] L. Dou, C. Song, X. Wang, L. Liu, and G. Feng, "Target localization and enclosing control for networked mobile agents with bearing measurements," *Automatica*, vol. 118, p. 109022, 2020.
- [13] J. Wang, B. Ma, and K. Yan, "Target circumnavigation of mobile robots using range-only measurements," *Automatica*, vol. 159, p. 111386, 2024.
- [14] F. Dong, Y. Hsu, and K. You, "Circumnavigation of an unknown target using range-only measurements in gps-denied environments," in *2019 IEEE 15th International Conference on Control and Automation (ICCA)*. IEEE, 2019, pp. 411–416.
- [15] A. S. Matveev, A. A. Semakova, and A. V. Savkin, "Range-only based circumnavigation of a group of moving targets by a non-holonomic mobile robot," *Automatica*, vol. 65, pp. 76–89, 2016.
- [16] A. S. Matveev and A. A. Semakova, "Range-only-based three-dimensional circumnavigation of multiple moving targets by a nonholonomic mobile robot," *IEEE Transactions on Automatic Control*, vol. 63, no. 7, pp. 2032–2045, 2017.
- [17] I. Shames, S. Dasgupta, B. Fidan, and B. D. Anderson, "Circumnavigation using distance measurements under slow drift," *IEEE Transactions on Automatic Control*, vol. 57, no. 4, pp. 889–903, 2011.
- [18] F. Liu, S. Yuan, K. Cao, W. Meng, and L. Xie, "Distance-based multiple noncooperative ground target encirclement for complex environments," *IEEE Transactions on Control Systems Technology*, 2024.
- [19] I. Shames, A. N. Bishop, and B. D. Anderson, "Analysis of noisy bearing-only network localization," *IEEE Transactions on Automatic Control*, vol. 58, no. 1, pp. 247–252, 2012.
- [20] J. Djughash, S. Singh, G. Kantor, and W. Zhang, "Range-only slam for robots operating cooperatively with sensor networks," in *Proceedings 2006 IEEE International Conference on Robotics and Automation, 2006. ICRA 2006*. IEEE, 2006, pp. 2078–2084.
- [21] J. Wang, B. Ma, and K. Yan, "Mobile robot circumnavigating an unknown target using only range rate measurement," *IEEE Transactions on Circuits and Systems II: Express Briefs*, vol. 69, no. 2, pp. 509–513, 2021.
- [22] A. Hashemi, Y. Cao, D. W. Casbeer, and G. Yin, "Unmanned aerial vehicle circumnavigation using noisy range-based measurements without global positioning system information," *Journal of Dynamic Systems, Measurement, and Control*, vol. 137, no. 3, p. 031003, 2015.
- [23] D. Milutinović, D. Casbeer, Y. Cao, and D. Kingston, "Coordinate frame free dubins vehicle circumnavigation using only range-based measurements," *International Journal of Robust and Nonlinear Control*, vol. 27, no. 16, pp. 2937–2960, 2017.
- [24] F. Dong, K. You, and S. Song, "Target encirclement with any smooth pattern using range-based measurements," *Automatica*, vol. 116, p. 108932, 2020.
- [25] F. Dong, K. You, L. Xie, and Q. Hu, "Coordinate-free circumnavigation of a moving target via a pd-like controller," *IEEE Transactions on Aerospace and Electronic Systems*, vol. 58, no. 3, pp. 2012–2025, 2021.
- [26] Y. Cao, J. Muse, D. Casbeer, and D. Kingston, "Circumnavigation of an unknown target using uavs with range and range rate measurements," in *52nd IEEE conference on decision and control*. IEEE, 2013, pp. 3617–3622.
- [27] P. Jain, C. K. Peterson, and R. W. Beard, "Encirclement of moving targets using noisy range and bearing measurements," *Journal of Guidance, Control, and Dynamics*, vol. 45, no. 8, pp. 1399–1414, 2022.
- [28] G. S. Bhati, A. Vaishnavi, and A. Jain, "Safe circumnavigation of a hostile target using range-based measurements," *arXiv preprint arXiv:2501.06528*, 2025. [Online]. Available: <http://arxiv.org/abs/2501.06528>
- [29] K. P. Tee, S. S. Ge, and E. H. Tay, "Barrier lyapunov functions for the control of output-constrained nonlinear systems," *Automatica*, vol. 45, no. 4, pp. 918–927, 2009.
- [30] A. Jain and D. Ghose, "Trajectory-constrained collective circular motion with different phase arrangements," *IEEE Transactions on Automatic Control*, vol. 65, no. 5, pp. 2237–2244, 2019.

- [31] A. Hegde and A. Jain, "Synchronization and balancing around simple closed polar curves with bounded trajectories," *Automatica*, vol. 149, p. 110810, 2023.
- [32] H. K. Khalil, *Control of nonlinear systems*. Prentice Hall, New York, NY, 2002.